

# Bremsstrahlung in $K \rightarrow \pi e^\pm \nu_e(\gamma)$ decays and Monte Carlo

Qingjun Xu<sup>a,b</sup> and Z. Was<sup>b,c</sup>

<sup>a</sup> *Department of Physics, Hangzhou Normal University, Hangzhou 310036, China*

<sup>b</sup> *Institute of Nuclear Physics, PAN, Kraków, ul. Radzikowskiego 152, Poland*

<sup>c</sup> *CERN PH-TH, CH-1211 Geneva 23, Switzerland*

## ABSTRACT

In physics simulation chains the PHOTOS Monte Carlo is often used in order to simulate QED effects in decays of intermediate particles and resonances. With the help of selection cuts, experimental acceptance can also be taken into account.

The program is based on an exact multiphoton phase space. However, the matrix element is obtained using kernel iterations, which involves approximations. To evaluate its precision, it is necessary to prepare and install into the generator the exact matrix element, which depends on the decay channel. As a consequence, all terms necessary for non-leading logarithms are taken into account. In the present paper we will focus on the decay  $K \rightarrow \pi l^\pm \nu_l$  and tests of the PHOTOS Monte Carlo program. We claim a 0.2% precision in the implementation of the hard photon matrix element into the emission kernel, also in case when approximations are used.

November 19, 2018

IFJPAN-IV-2011-14  
CERN-PH-TH/2011-309  
December, 2011

---

<sup>†</sup> Work of ZW is supported in part by the Polish Ministry of Science and Higher Education grant No. 1289/B/H03/2009/37.

# 1 Introduction

Semileptonic flavour changing decays, such as  $K \rightarrow \pi l \nu_l$  offer a window for measurements of Standard Model basic couplings: quark mixing angles [1]. Moreover properties of low and medium energy hadronic interactions manifest themselves in such decays. It is thus of importance to keep control of decay products distributions in a form suitable for comparisons with data and without loosing control of the underlying quark level matrix element.

Without question, the comparison between experimental data and theory, must rely on Monte Carlo simulation, as it necessitates taking into account the detector response [2]. Given the present day experimental precision, generators used in comparisons must be based on exact phase space and explicit form of the matrix element. Otherwise the discussion of theoretical uncertainties in realistic applications is rather difficult.

QED bremsstrahlung must be taken into account in these comparisons too. Infrared singularities cancel out in sufficiently inclusive observables. In a first approximation QED bremsstrahlung amplitude can be factorized into Born amplitude and emission (eikonal or collinear) term. This can be done for calculation at a fixed order, but it holds to all orders and is known under the name of exponentiation [3] (for Monte Carlo application see e.g. [4, 5]). Also, in phase-space regions where photons are collinear to charged particles, factorization theorems define the dominant terms of the amplitudes. This is why, bremsstrahlung can be treated to a good precision independently of the decay channel. As a consequence predictions, which neglect QED effects, represent a valid segment of the phenomenology work.

For the decays of a given particle, matrix elements based Monte Carlo generators are prepared either by theorists working on effective lagrangians (also on QCD based predictions), or by experimental physicists who are going to use the programs. Let us return now to QED. Since many years PHOTOS Monte Carlo is used [6, 7] for simulation in experimental applications of bremsstrahlung in decays, and it represent a separate segment of the simulation chain.

With the increased precision of presently arriving data, such an arrangement requires a careful discussion of its systematic errors, which has to be repeated separately for each decay mode. The phenomenological importance of approximations needs to be analyzed, and the factorization of QED need to be reviewed, using as a reference solutions based on exact phase-space and matrix element for the whole decay (thus including QED bremsstrahlung).

In Ref. [6] PHOTOS Monte Carlo was presented for the first time. The universal kernel was introduced and was shown to work well in several cases when comparisons with first order matrix element reference simulation programs were available. In papers [7] and [8] iteration was introduced into PHOTOS Monte Carlo. First, for double photon emission, and later for multiple photon emission as well. Because of a rather unique order of iteration (iteration over sources providing collinear singularities is performed first, and only later on consecutive photons are constructed), the algorithm is compatible at the same time with exclusive exponentiation and resummation of collinear logarithms.

In paper [9] a discussion of the exact matrix element implemented into the PHOTOS kernel was performed for the  $Z$  decay. The discussion was continued in Ref. [10] for the

decay of a scalar into pair of scalars. In that paper, a detailed presentation of the phase space parametrization was given as well. It was followed in [11] with a discussion of matrix elements for the  $W$  leptonic decay and the decay of virtual photons to pairs of scalars. With [12] matrix element weights became available for the public use.

Until now, discussions of matrix elements were concentrated on two-body decays only. In that case, not only phase space at Born level is particularly simple, but also photon emission is simpler to handle as well.

In the present paper, we will turn our attention to the decay  $K_{l3}$  for which already at the Born level a three-body kinematic is present. By studying this decays, we will test not only effects of the matrix element implementation, but also PHOTOS phase-space generation<sup>1</sup>.

Our paper is organized as follows. In Section 2 we present the matrix elements for  $K_{l3}$  decays, at Born level and for the case of single photon emission. Results of calculations based on scalar QED [13] and on ChPT [14, 15, 16] with truncations as in Refs. [17, 18] will be compared and discussed. In this context we also investigate, matrix elements and their factorization properties. In Section 3, we turn our attention to fully differential distributions. For that purpose squared matrix element are reviewed and possible options resulting from physics assumptions (scalar QED or [17, 18]) are shown. We address again factorization properties, this time in context of features which are useful for Monte Carlo. Our set-up and arrangements prepared for tests are presented in Section 4. Numerical results are collected in Section 5. Conclusions, including the estimation of PHOTOS Monte Carlo precision for the  $K_{l3}$  decays, are given in Section 6.

## 2 Amplitudes for $K_{l3}(\gamma)$ decays.

Let us start our discussion from the amplitude of the decay

$$K^-(p) \rightarrow \pi^0(q) + e^-(p_e) + \nu(p_\nu) \quad (1)$$

taken at the Born level. With the notation of Ref. [17, 18] it reads

$$M_{\text{Born}}^c = \frac{e^2 V_{us}^* F_{K\pi}(t)}{8\sqrt{2}s_W^2} \frac{(p+q)^\mu}{t - M_W^2} \bar{u}(p_e, \lambda_e) \gamma_\mu (1 - \gamma_5) v(p_\nu, \lambda_\nu), \quad (2)$$

where  $\lambda_e, \lambda_\nu$  denote helicities of electron and neutrino,  $F_{K\pi}(t)$  is the form factor and  $t = (p - q)^2$ . Because of the relatively small mass of the  $K$  meson,  $t$  is always  $\ll M_W^2$  and the

---

<sup>1</sup>Parametrization of phase-space in PHOTOS is explicit and exact, if the presampler for collinear emissions is used only along a single charge. Otherwise, starting from the moment when the photon is supposed to be added to a more than two-body configuration, an approximation appears when the phase-space Jacobians for the multitude of branches are combined. This can be improved, but for test cases with second order matrix elements in  $Z$  decay [9], we have found that this approximation is necessary, unless complete double photon emission amplitude would be installed into the program at the same time.

amplitude simplifies to

$$M_{\text{Born}}^c = \frac{G_F V_{us}^* F_{K\pi}(t)}{2} (p+q)^\mu \bar{u}(p_e, \lambda_e) \gamma_\mu (1 - \gamma_5) v(p_\nu, \lambda_\nu). \quad (3)$$

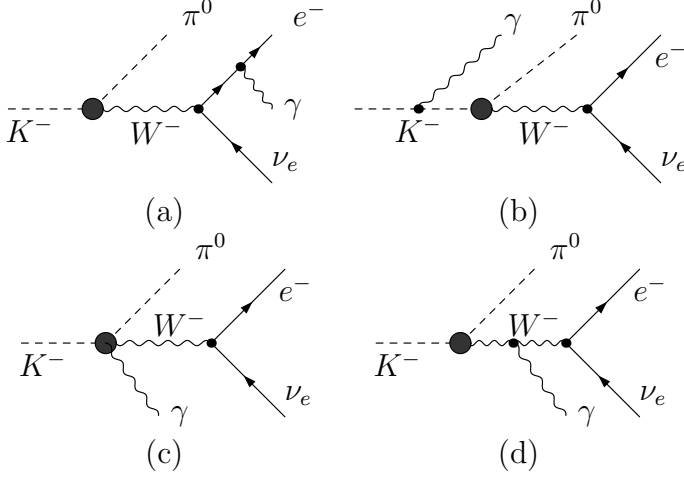


Figure 1: Feynman diagrams of  $K^- \rightarrow \pi^0 e^- \nu \gamma$

Let us now turn to amplitudes for single photon emission. We follow Ref. [11] and we define photon polarization states in the rest frame of the  $K$  meson. This choice fix the gauge. However, in the following our amplitudes are formulated in a Lorentz and gauge invariant way.

Scalar QED diagrams for  $K^-(p) \rightarrow \pi^0(q) e^-(p_e) \nu(p_\nu) \gamma(k)$  decay are presented in Figure 1. The contribution of diagram (d) is proportional to  $1/M_W^4$  while for other diagrams it is proportional to  $1/M_W^2$ . For this reason, we can neglect the contribution of (d). The amplitude for  $K^- \rightarrow \pi^0 e^- \nu \gamma$  reads:

$$M^c = \frac{G_F V_{us}^* F_{K\pi}(t)}{2} \bar{u}(p_e, \lambda_e) \left[ Q_e (p+q)^\mu \left( \frac{p_e \cdot \epsilon}{p_e \cdot k} + \frac{\not{\epsilon} \not{k}}{2 p_e \cdot k} \right) - Q_K (p+q-k)^\mu \frac{p \cdot \epsilon}{p \cdot k} - Q_k \epsilon^\mu \right] \gamma_\mu (1 - \gamma_5) v(p_\nu, \lambda_\nu), \quad (4)$$

where  $Q_e, Q_K$  denote the charges, respectively of  $e^-$  and  $K^-$ . To visualize the factorization properties this amplitude can be separated into a sum of three gauge invariant parts:

$$M^c = M_I^c + M_{II}^c + M_{III}^c, \quad (5)$$

where

$$M_I^c = \frac{G_F V_{us}^* F_{K\pi}(t)}{2} (p+q)^\mu \left( Q_e \frac{p_e \cdot \epsilon}{p_e \cdot k} - Q_K \frac{p \cdot \epsilon}{p \cdot k} \right) \bar{u}(p_e, \lambda_e) \gamma_\mu (1 - \gamma_5) v(p_\nu, \lambda_\nu), \quad (6)$$

$$M_{II}^c = \frac{G_F V_{us}^* F_{K\pi}(t)}{2} (p+q)^\mu \bar{u}(p_e, \lambda_e) Q_e \frac{\not{\epsilon} \not{k}}{2 p_e \cdot k} \gamma_\mu (1 - \gamma_5) v(p_\nu, \lambda_\nu), \quad (7)$$

$$M_{III}^c = \frac{G_F V_{us}^* F_{K\pi}(t)}{2} Q_k \left( k^\mu \frac{p \cdot \epsilon}{p \cdot k} - \epsilon^\mu \right) \bar{u}(p_e, \lambda_e) \gamma_\mu (1 - \gamma_5) v(p_\nu, \lambda_\nu). \quad (8)$$

The first part  $M_I^c$  consists of Born-level amplitude times an eikonal factor. The second,  $M_{II}^c$ , is free of soft singularity but grows logarithmically in the collinear limit. Finally the third part,  $M_{III}^c$ , is free of both soft and collinear singularities. Hence, formula (5) provides a clearly structured expression of the amplitude.

For each term (6,7,8) a separation into leptonic and hadronic terms is manifest. It is encouraging, because it coincides with the structure of separation we have observed in [11], which was useful for our discussion there. Again, we see that the first two parts are process independent in their emission aspect, and only the last non-dominant part breaks this property<sup>2</sup>. This is why, we expect this formulation to be useful for our numerical discussion.

Let us now turn to comparison with amplitudes of Ref. [17]. Our Born and photon emission amplitudes, formulae (3) and (4), thanks to Dirac equation take the forms:

$$M_{\text{Born}}^c = \frac{G_F V_{us}^* F_{K\pi}(t)}{2} \bar{u}(p_e, \lambda_e) (2 \not{q} + m_e) (1 - \gamma_5) v(p_\nu, \lambda_\nu) \quad (9)$$

and

$$M^c = \frac{G_F V_{us}^* F_{K\pi}(t)}{2} \bar{u}(p_e, \lambda_e) \left[ \left( Q_e \frac{p_e \cdot \epsilon}{p_e \cdot k} - Q_K \frac{p \cdot \epsilon}{p \cdot k} \right) + Q_e \frac{\not{\epsilon} \not{k}}{2 p_e \cdot k} \right] (2 \not{q} + m_e) (1 - \gamma_5) v(p_\nu, \lambda_\nu). \quad (10)$$

This new formulation coincide with formula (13) of Ref. [17]. Because of consistency of expansion, the form factor is taken at  $t = 0$  in Ref. [17] (see there, formulae (2) and (3)), we follow the same choice.

The new form of the amplitude can be also splitted into two gauge invariant parts:

$$M^c = M_{I'}^c + M_{II'}^c \quad (11)$$

$$M_{I'}^c = \frac{G_F V_{us}^* F_{K\pi}(t)}{2} \bar{u}(p_e, \lambda_e) \left( Q_e \frac{p_e \cdot \epsilon}{p_e \cdot k} - Q_K \frac{p \cdot \epsilon}{p \cdot k} \right) (2 \not{q} + m_e) (1 - \gamma_5) v(p_\nu, \lambda_\nu), \quad (12)$$

$$M_{II'}^c = \frac{G_F V_{us}^* F_{K\pi}(t)}{2} \bar{u}(p_e, \lambda_e) Q_e \frac{\not{\epsilon} \not{k}}{2 p_e \cdot k} (2 \not{q} + m_e) (1 - \gamma_5) v(p_\nu, \lambda_\nu). \quad (13)$$

The first gauge invariant part has the form of a born-like amplitude times an eikonal factor. The second one does not contribute to soft singularities, but contribute to collinear singularities. Unfortunately formulae (12, 13) do not hold the universal, process independent form.

For all amplitudes presented above as well as their parts, the terms proportional to the electron mass were carefully kept. This is why we can extend our results to the case of the  $K^- \rightarrow \pi^0 \mu^- \nu_\mu$  decay as well.

## 2.1 Amplitude for $K^0(p) \rightarrow \pi^+(q) + e^-(p_e) + \nu(p_\nu)$ decay

Let us now turn to  $K_{l3}$  decay of the neutral  $K$ :  $K^0(p) \rightarrow \pi^+(q) + e^-(p_e) + \nu(p_\nu)$ . This channel is interesting from the point of view of Monte Carlo discussions, even though is not

---

<sup>2</sup>Expression (8) coincide also with analogous part (19) of discussed later amplitude for the  $K^0 \rightarrow \pi^\mp l^\pm \nu_l$  decay.

of large phenomenological relevance. There are not only two charged particles of different masses in the final state, but they are also accompanied by a neutral  $\nu$ . This is interesting from the point of view of phase space generation.

The charged and neutral  $K$  decays amplitudes are quite similar. The Born level amplitude reads:

$$M_{\text{Born}}^0 = \frac{G_F V_{us}^* F_{K\pi}(t)}{\sqrt{2}} (p+q)^\mu \bar{u}(p_e, \lambda_e) \gamma_\mu (1 - \gamma_5) v(p_\nu, \lambda_\nu). \quad (14)$$

The amplitude for single photon emission is again quite short

$$M^0 = \frac{G_F V_{us}^* F_{K\pi}(t)}{\sqrt{2}} \bar{u}(p_e, \lambda_e) \left[ Q_e (p+q)^\mu \left( \frac{p_e \cdot \epsilon}{p_e \cdot k} + \frac{\not{\epsilon} \not{k}}{2p_e \cdot k} \right) + Q_\pi (p+q+k)^\mu \frac{p \cdot \epsilon}{p \cdot k} - Q_\pi \epsilon^\mu \right] \gamma_\mu (1 - \gamma_5) v(p_\nu, \lambda_\nu). \quad (15)$$

and can be separated into sum of three gauge invariant parts:

$$M^0 = M_I^0 + M_{II}^0 + M_{III}^0, \quad (16)$$

where

$$M_I^0 = \frac{G_F V_{us}^* F_{K\pi}(t)}{\sqrt{2}} (p+q)^\mu \left( Q_e \frac{p_e \cdot \epsilon}{p_e \cdot k} + Q_\pi \frac{q \cdot \epsilon}{q \cdot k} \right) \bar{u}(p_e, \lambda_e) \gamma_\mu (1 - \gamma_5) v(p_\nu, \lambda_\nu), \quad (17)$$

$$M_{II}^0 = \frac{G_F V_{us}^* F_{K\pi}(t)}{\sqrt{2}} (p+q)^\mu \bar{u}(p_e, \lambda_e) Q_e \frac{\not{\epsilon} \not{k}}{2p_e \cdot k} \gamma_\mu (1 - \gamma_5) v(p_\nu, \lambda_\nu), \quad (18)$$

$$M_{III}^0 = \frac{G_F V_{us}^* F_{K\pi}(t)}{\sqrt{2}} Q_\pi \left( k^\mu \frac{q \cdot \epsilon}{q \cdot k} - \epsilon^\mu \right) \bar{u}(p_e, \lambda_e) \gamma_\mu (1 - \gamma_5) v(p_\nu, \lambda_\nu). \quad (19)$$

The  $Q_\pi$  denotes the  $\pi^\pm$  charge. As in the case of  $K^\pm$  only the first part, formula (17), is infrared singular, and the third part is free of collinear singularity.

With the help of the Dirac equation we can transform (15) into:

$$M^0 = \frac{G_F V_{us}^* F_{K\pi}(t)}{\sqrt{2}} \bar{u}(p_e, \lambda_e) \left[ \left( Q_e \frac{p_e \cdot \epsilon}{p_e \cdot k} + Q_\pi \frac{q \cdot \epsilon}{q \cdot k} \right) + Q_e \frac{\not{\epsilon} \not{k}}{2p_e \cdot k} \right] (2 \not{k} + m_e) (1 - \gamma_5) v(p_\nu, \lambda_\nu) + 2 \frac{G_F V_{us}^* F_{K\pi}(t)}{\sqrt{2}} Q_\pi \left( k^\mu \frac{q \cdot \epsilon}{q \cdot k} - \epsilon^\mu \right) \bar{u}(p_e, \lambda_e) \gamma_\mu (1 - \gamma_5) v(p_\nu, \lambda_\nu), \quad (20)$$

which has the same form as in Ref. [17]. However our expression does not coincide with formula (14) of Ref. [17]. In Ref. [17] only the first term of our formula (20) is present, and in our notations formula (14) of Ref. [17] reads:

$$M_{I'}^0 = \frac{G_F V_{us}^* F_{K\pi}(t)}{\sqrt{2}} \bar{u}(p_e, \lambda_e) \left[ \left( Q_e \frac{p_e \cdot \epsilon}{p_e \cdot k} + Q_\pi \frac{q \cdot \epsilon}{q \cdot k} \right) + Q_e \frac{\not{\epsilon} \not{k}}{2p_e \cdot k} \right] (2 \not{k} + m_e) (1 - \gamma_5) v(p_\nu, \lambda_\nu). \quad (21)$$

Formula (21) is not consistent with a leading logarithm approximation for a photon emission collinear with  $\pi^\pm$ . On the other hand, for the  $K^0$  decay there is no collinear enhancement of photon emission along direction of  $\pi^\pm$  because it is not ultrarelativistic. This is why the inconsistency has no practical consequences. It is nonetheless an interesting observation. The case is quite similar to the one of Ref. [11]; (formulas (11) and (13) there) and is rather simple to fix: improved in that respect formula (14) of Ref. [17] would read:

$$M_{I''}^0 = \frac{G_F V_{us}^* F_{K\pi}(t)}{\sqrt{2}} \bar{u}(p_e, \lambda_e) \left[ \left( Q_e \frac{p_e \cdot \epsilon}{p_e \cdot k} + Q_\pi \frac{q \cdot \epsilon}{q \cdot k} \right) \left( 2 \left( \not{q} + \not{k} \frac{p_e \cdot k}{q \cdot k + p_e \cdot k} \right) + m_e \right) + Q_e \frac{\not{\epsilon} \not{k}}{2 p_e \cdot k} (2 \not{q} + m_e) \right] (1 - \gamma_5) v(p_\nu, \lambda_\nu). \quad (22)$$

We will use it also. Our motivation is purely technical: we want to investigate it numerically in comparisons, for bremsstrahlung in neutral  $K_{l3}$  decays as another option for matrix element. It may be of importance for the case of  $B_{l3}$  decays.

Our formula (20) can be re-written also as a sum of  $M_{I''}^0$  and of  $M_{II'}^0$ :

$$\begin{aligned} M_0 &= M_{I''}^0 + M_{II'}^0, \\ M_{II'}^0 &= 2 \frac{G_F V_{us}^* F_{K\pi}(t)}{\sqrt{2}} \left( \frac{k^\mu}{q \cdot k + p_e \cdot k} (Q_\pi q \cdot \epsilon + Q_e p_e \cdot \epsilon) - Q_\pi \epsilon^\mu \right) \bar{u}(p_e, \lambda_e) \gamma_\mu (1 - \gamma_5) v(p_\nu, \lambda_\nu), \end{aligned} \quad (23)$$

where  $M_{II'}$  is free of singularities.

### 3 Spin averaged amplitude squares.

The spin states of the  $K_{l3}$  decay products are not measurable. Our interest is thus limited to differential distributions. For that purpose spin summed squares of the amplitudes are the natural object to study. In the present Section we will explore squares of amplitudes given by eqs. (12, 13).

In the following, we will use the following notations:

$$S = 2p_e \cdot p_\nu, T = 2q \cdot p_e, U = 2q \cdot p_\nu. \quad (24)$$

Let us start with the Born level expression for the charged  $K$  decay:

$$\begin{aligned} \sum |M_{\text{Born}}^c|^2 &= \frac{G_F^2 |V_{us}|^2 F_{K\pi}(t)^2}{4} \times 32 \times \left[ q \cdot p_\nu (2q \cdot p_e + m_e^2) - \left( m_\pi^2 - \frac{m_e^2}{4} \right) p_\nu \cdot p_e \right] \\ &= \frac{G_F^2 |V_{us}|^2 F_{K\pi}(t)^2}{4} \times 16 \times \left[ U (T + m_e^2) - \left( m_\pi^2 - \frac{m_e^2}{4} \right) S \right]. \end{aligned} \quad (25)$$

For the bremsstrahlung case, the square of the amplitude reads

$$\sum |M^c|^2 = \sum |M_{I'}^c|^2 + \sum |M_{II'}^c|^2 + 2 \sum M_{I'}^c M_{II'}^{c*}, \quad (26)$$

where

$$\begin{aligned} \sum |M_{I'}^c|^2 &= 32 \sum_{i=1,2} \left( Q_e \frac{p_e \cdot \epsilon_i}{p_e \cdot k} - Q_K \frac{p \cdot \epsilon_i}{p \cdot k} \right)^2 \\ &\quad \frac{G_F^2 |V_{us}|^2 F_{K\pi}(t)^2}{4} \left[ q \cdot p_\nu (2q \cdot p_e + m_e^2) - \left( m_\pi^2 - \frac{m_e^2}{4} \right) p_\nu \cdot p_e \right], \end{aligned} \quad (27)$$

$$\begin{aligned} \sum |M_{II'}^c|^2 &= \frac{-16Q_e^2}{p_e \cdot k} \sum_{i=1,2} (\epsilon_i \cdot \epsilon_i) \frac{G_F^2 |V_{us}|^2 F_{K\pi}(t)^2}{4} \left[ 2q \cdot p_\nu q \cdot k - \left( m_\pi^2 - \frac{m_e^2}{4} \right) p_\nu \cdot k \right] \\ &\quad (28) \end{aligned}$$

$$\begin{aligned} 2 \sum M_{I'}^c M_{II'}^{c*} &= 32 \frac{G_F^2 |V_{us}|^2 F_{K\pi}(t)^2}{4} \\ &\quad \left[ \sum_{i=1,2} Q_e \frac{p_e \cdot \epsilon_i}{p_e \cdot k} \left( Q_e \frac{p_e \cdot \epsilon_i}{p_e \cdot k} - Q_K \frac{p \cdot \epsilon_i}{p \cdot k} \right) \left( 2q \cdot p_\nu q \cdot k - \left( m_\pi^2 - \frac{m_e^2}{4} \right) p_\nu \cdot k \right) \right. \\ &\quad \left. - \sum_{i=1,2} Q_e \left( Q_e \frac{p_e \cdot \epsilon_i}{p_e \cdot k} - Q_K \frac{p \cdot \epsilon_i}{p \cdot k} \right) \left( 2q \cdot p_\nu q \cdot \epsilon_i - \left( m_\pi^2 - \frac{m_e^2}{4} \right) p_\nu \cdot \epsilon_i \right) \right]. \end{aligned} \quad (29)$$

Here  $\epsilon_1, \epsilon_2$  are two orthogonal photon polarization vectors. As expected  $\sum |M_{I'}^c|^2$  consist of a Born-like expression multiplied by an eikonal factor. The second and third terms,  $\sum |M_{II'}^c|^2$  and  $2 \sum M_{I'}^c M_{II'}^{c*}$ , are free of soft singularities.

Formulae for neutral  $K$  decay  $K^0 \rightarrow \pi^+ e^- \nu_e$  are similar. One obtain from formula (14)

$$\sum |M_{\text{Born}}^0|^2 = 2 \times \sum |M_{\text{Born}}^c|^2. \quad (30)$$

It differs from the Born contribution of charged  $K$  decay by a factor of 2. For the bremsstrahlung case, the amplitude squared can be again separated into parts. The first



one consist of the squared formula (22)<sup>3</sup>, which reads:

$$\begin{aligned}
\sum |M_{I''}^0|^2 &= 2 \times \sum_{Q_k \rightarrow -Q_\pi, \frac{p \cdot \epsilon_i}{p \cdot k} \rightarrow \frac{q \cdot \epsilon_i}{q \cdot k}} |M^c|^2 \\
&+ 32 \frac{G_F^2 |V_{us}|^2 F_{K\pi}(t)^2}{2} \frac{p_e \cdot k}{q \cdot k + p_e \cdot k} \times \left[ \sum_{i=1,2} \left( Q_e \frac{p_e \cdot \epsilon_i}{p_e \cdot k} + Q_\pi \frac{q \cdot \epsilon_i}{q \cdot k} \right)^2 \right. \\
&\times \left( k \cdot p_\nu (2q \cdot p_e + m_e^2) + 2 \left( q \cdot p_\nu + \frac{p_e \cdot k}{q \cdot k + p_e \cdot k} k \cdot p_\nu \right) k \cdot p_e - 2q \cdot k p_\nu \cdot p_e \right) \\
&\left. + \sum_{i=1,2} 2Q_e \left( Q_e \frac{p_e \cdot \epsilon_i}{p_e \cdot k} + Q_\pi \frac{q \cdot \epsilon_i}{q \cdot k} \right) (p_\nu \cdot \epsilon_i q \cdot k - q \cdot \epsilon_i p_\nu \cdot k) \right]. \quad (32)
\end{aligned}$$

The second part, contributing to the squared amplitude for neutral  $K$  decay, consists of the squared formula (23) and its interference with formula (22). We do not write explicitly this expression here, as it is rather lengthy, and is also numerically rather small.

### 3.1 Virtual corrections

Virtual corrections for our decays can be found eg. in Ref. [17], they are of lesser importance and we will not recapitulate them here. The present work is devoted to the discussion of real emission corrections, which are detector selection depended. Virtual corrections have to be divided into two parts. One part which is large, but in total rate sums to zero with real emissions thanks to Kinoshita-Lee-Nauenberg theorem. This part is taken into account by PHOTOS Monte Carlo. The other part has to be included into the form-factor and incorporated into the Born level matrix element. For this purpose, real emission amplitude squared will need to be integrated over photon momentum to control the sum rule to the level of complete first order. This can be performed in an approximate way (as in Ref. [19])<sup>4</sup> or in an exact manner, following phase space parametrization as used in PHOTOS. Integration (analytic or numerical) will need to be performed. This solution has to be followed, once experimental precision approaches  $\frac{\alpha}{\pi}$  precision level. Other phase-space organization for Monte Carlo may be useful for that purpose. We will return to this point in the next section's footnote.

## 4 Monte Carlo

We use TAUOLA [20] to generate Born level decay samples. This generator is suitable for our purpose once the  $\tau$  decay matrix element is replaced with the one of the  $K_{l3}$

---

<sup>3</sup>It can be also obtained from formula (27,28,29) with the help of the change of variables

$$Q_k \rightarrow -Q_\pi, \quad \frac{p \cdot \epsilon_i}{p \cdot k} \rightarrow \frac{q \cdot \epsilon_i}{q \cdot k}. \quad (31)$$

<sup>4</sup>But then, no gain beyond Konoshita-Lee-Nauenberg can be achieved. In  $K_{e3}$  decay there is no Coulomb effect.

decay, and appropriate adjustment of masses and particle identifiers are performed as well. Semileptonic decays of  $\tau$ 's are suitable for such adaptation<sup>5</sup>. Another advantage is that we can then guarantee full control of parameters used in our Born level generator and in matrix element of PHOTOS correcting weights.

We gain also from the practical side. PHOTOS is ready to use with TAUOLA. Also, its interface to HEPEVT event record offers an easy access to our testing tool MC-TESTER [21, 22]. The prepared plots will be then compatible with our previous works as well. From the user point of view, numerical results collected for this paper, and available also in graphic form from the web-page [23], can be of interest for benchmarking  $K$  decay generators independently, whether they are implemented in FORTRAN or in C++.

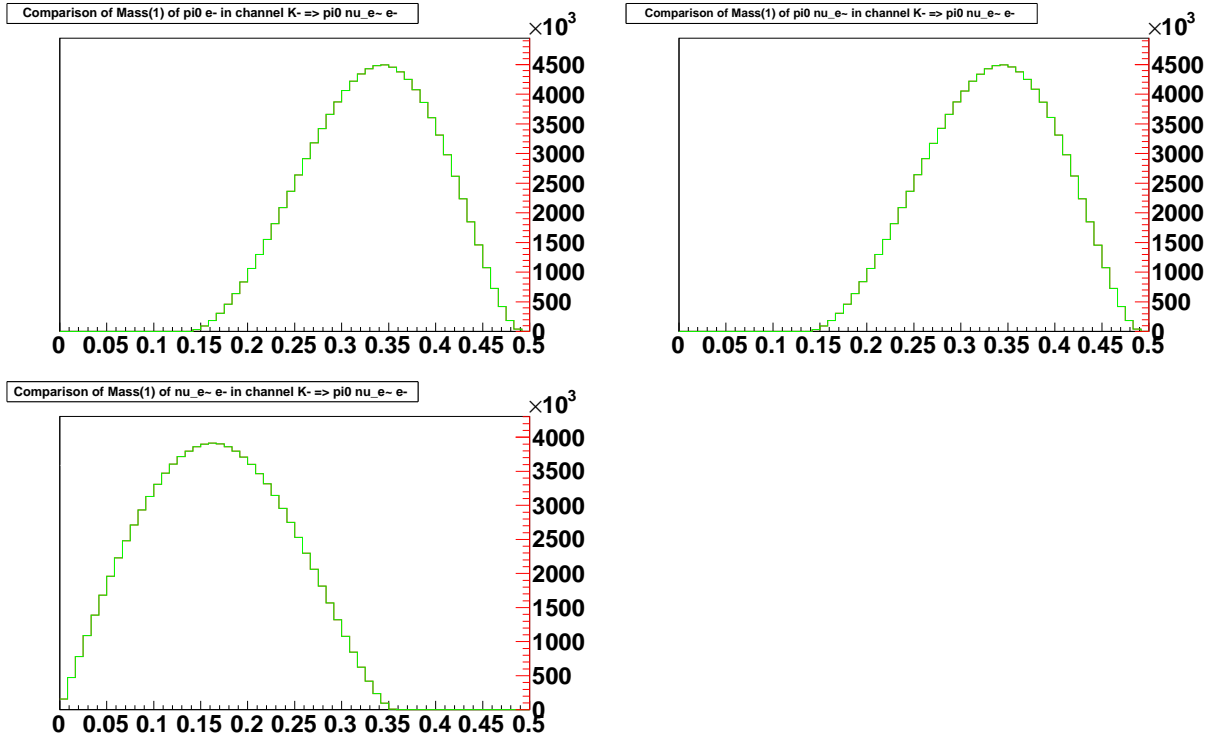


Figure 2: Distributions of invariant masses, in GeV units, constructed from the products of the decay  $K^- \rightarrow \pi^0 e^- \nu_e$ , at Born level. As in [24]  $V_{us} = 0.2246$  is used, we take however  $F_{K\pi}(t) = 1$ . This is an acceptable approximation for our purposes.

The squares of Born level amplitudes (25) for decays  $K^- \rightarrow \pi^0 e^- \nu_e$ , and  $K^0 \rightarrow \pi^+ e^- \nu_e$  are rather easy to implement into TAUOLA. The numerical results, as histograms of invariant masses constructed from pairs of final state decay products, are shown in Fig. 2. We have compared these results with the one of Ref. [25] and obtained an agreement. This comparison is sufficient for tests, because the matrix element is rather simple and TAUOLA

<sup>5</sup> TAUOLA semileptonic decay channel offer an alternative crude phase space generator for radiative corrections, which may become useful in the future for technical tests, especially if complete virtual corrections are to be included and studied.

itself is well tested. Note that detector acceptance effects were taken into account in Ref. [25], for this reason figures of that paper will not coincide in all details with our Fig. 2.

## 5 Numerical results

In all tests presented in this paper we use samples of 100 Mevts. In our tests, we will refer to standard PHOTOS whenever we will use its publicly available FORTRAN version 2.15, or any other version which yields equivalent results. In particular, identical results are available from the C++ PHOTOS [26], version 3.0 or 3.3. One of the goals of the paper is to provide an estimation of the systematic error for these widely used versions. As a first step, we perform a technical test.

For the decay of charged  $K$  we have compared results of the standard PHOTOS with the PHOTOS version of [10]. That was the first version where the phase space generation for final state of a single charged particle was exact, which was provided with the help of explicit phase space Jacobians. It is publicly available starting from PHOTOS++, version 3.3. We could see that the numerical effect is small. As expected, the difference is below 0.05 % if calculated with respect to the total rate. We obtained differences at the level of 10 % in regions of phase space contributing at the level of  $10^{-4}$  to the total rate. We have checked the contribution from collinear photon emission region. To this end we have selected only those events, used in the previous comparison, where invariant mass of photon-electron pair was at most 0.01 of their energies product (taken in the rest frame of  $K$ ). We obtained perfect agreement, with no statistically significant differences.

Throughout the paper, we use our testing program MC-TESTER [21, 22]. The two colored (grey) lines correspond to the compared generation samples, whereas the black line represents their ratio. The SDP (shape difference parameter) also obtained from MC-TESTER represents an exclusive surface (normalized to unity) under the green and red distributions. We subtract the statistical error from the difference. The distributions of Lorentz invariants constructed from outgoing particles are shown.

We have repeated the same comparison as discussed previously but when the complete matrix element is installed. As we can see from Fig. 3 the numerical effect of the Matrix Element and exact phase space implementation is rather small, only at the ends of the spectra (contributing at the level of  $10^{-3}$  to the total rate) relative differences are sizable. There, matrix element effects are rather substantial and should be kept in mind in some contexts, e.g. for generating background to other decays.

For the case of  $K^- \rightarrow \pi^0 \mu^- \nu_\mu$ , logarithmic corrections are of course much smaller. That is why non leading terms contribute to photon spectra in a relatively larger manner, and seemingly much larger effects can be seen in Fig. 4 than in Fig. 3. Nonetheless it is not more significant numerically. Only 0.45 % of events enter the plots for the muonic channel; twenty times less than in the electron case. We can conclude that standard PHOTOS work sufficiently well for the  $K^- \rightarrow \pi^0 \mu^- \nu_\mu$  decay, if one is interested in 0.2 % precision limits.

Let us now turn to the  $K^0 \rightarrow \pi^+ l^- \nu_l$  case. It is technically more interesting as two

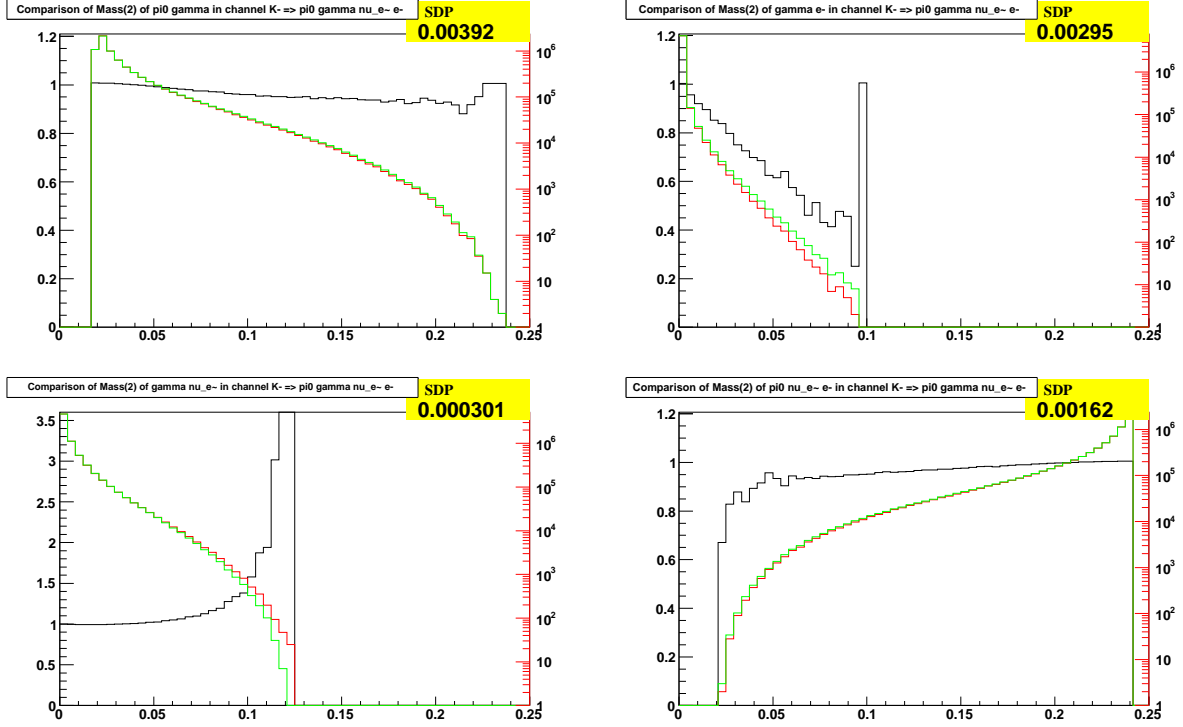


Figure 3: Distributions of scalar Lorentz invariants, in  $\text{GeV}^2$  units, constructed from the decay products in  $K^- \rightarrow \pi^0 e^- \nu_e$  channel. Invariants most sensitive to photon energy are plotted. The red (darker grey) line is standard PHOTOS, the green is with exact Matrix Element, both correspond to the right logarithmic scale. The black line is ratio of red to green, and correspond to the left linear scale. The fraction of accepted bremsstrahlung events is  $7.371 \pm 0.0027 \%$  in standard PHOTOS run and  $7.4127 \pm 0.0027 \%$  for the case where the matrix element is used.

kinematical branches are present in the crude level phase-space generator.

In Fig. 5 we compare standard PHOTOS with the one where the matrix element is installed. The approximation in the phase space is still present. Only in Fig. 6 we use single channel presampler for the phase-space generation and the phase space is exact. Note, that the effect of phase space Jacobian approximation is rather small.

By comparing Figs. 7 and 6 we can see that the standard PHOTOS is much closer to the result of scalar QED matrix element than to one of Ref. [17]. The bulk of the difference is due to non-compatibility of formulae from [17] with collinear logarithms due to emission from charged pion (we can see it by comparing Fig. 8 as well). This is of course beyond the framework of approximation claimed in Ref. [17], but it is nonetheless of some interest to understand the origin of the residual differences with respect to e.g. scalar QED.

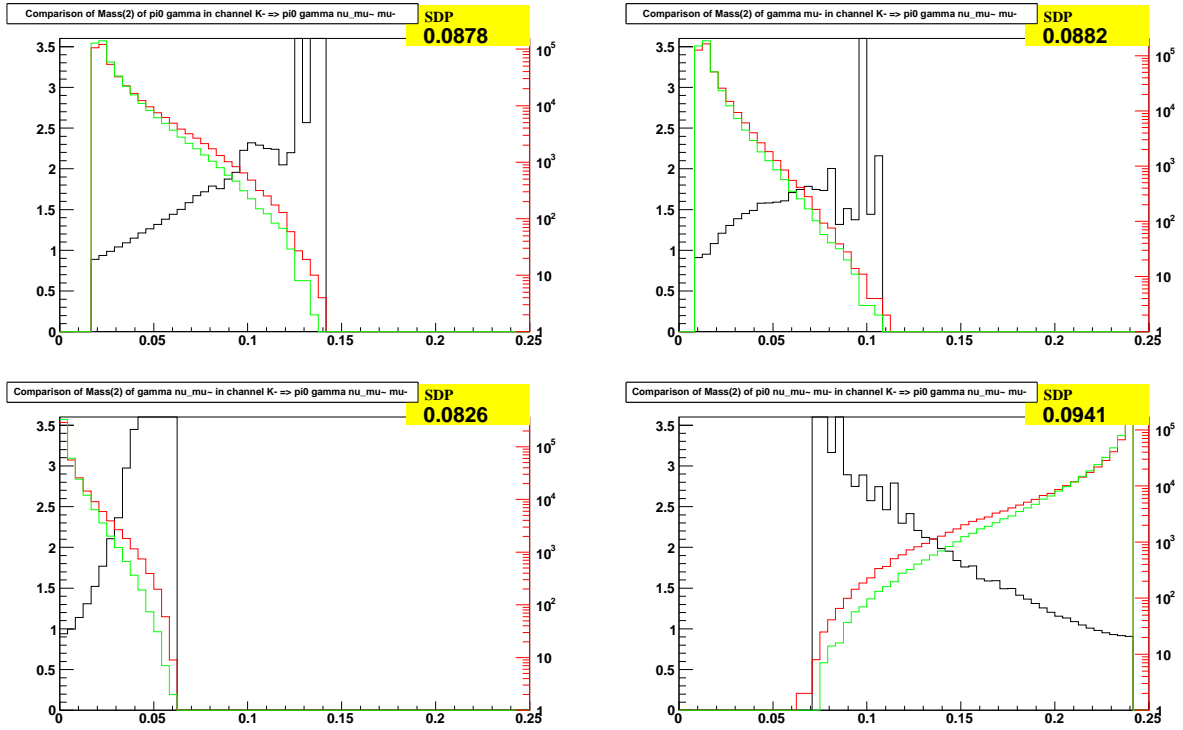


Figure 4: Distributions of scalar Lorentz invariants, in  $\text{GeV}^2$  units, constructed from the decay products in  $K^- \rightarrow \pi^0 \mu^- \nu_\mu$  channel. Invariants most sensitive to photon energy are shown. The red (darker grey) line is standard PHOTOS, the green is with exact Matrix Element, both correspond to the right logarithmic scale. The black line is ratio of red to green, and correspond to the left linear scale. One could conclude that effect of matrix element introduction is not small in this case. However, only a small fraction of events enter this plot  $0.4113 \pm 0.0006 \%$  for standard standard PHOTOS and  $0.4445 \pm 0.0007 \%$  for the case with matrix element. The difference is well below  $0.1 \%$  when compared to the total rate. The two distributions coincide in the soft photon region.

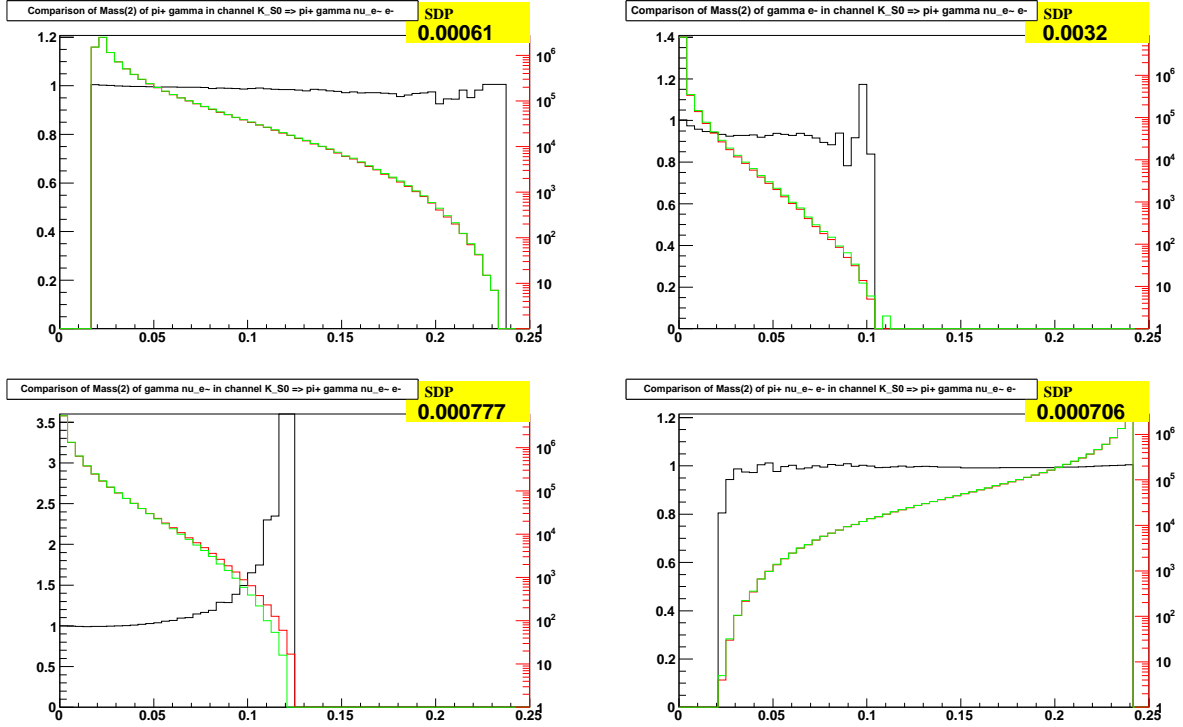


Figure 5: Distributions of scalar Lorentz invariants, in  $\text{GeV}^2$  units, constructed from the decay products in  $K^0 \rightarrow \pi^+ e^- \nu_e$  channel. Invariants most sensitive to photon energy are plotted. Two kinematical branches are used, thus the phase space is not exact. The red (darker grey) line is standard PHOTOS, the green is with exact Matrix Element, both correspond to the right logarithmic scale. The black line is ratio of red to green, and correspond to the left linear scale. The fraction of accepted bremsstrahlung events is  $8.6398 \pm 0.0029 \%$  in standard PHOTOS run and  $8.6913 \pm 0.0029 \%$  for the case where the matrix element is used.

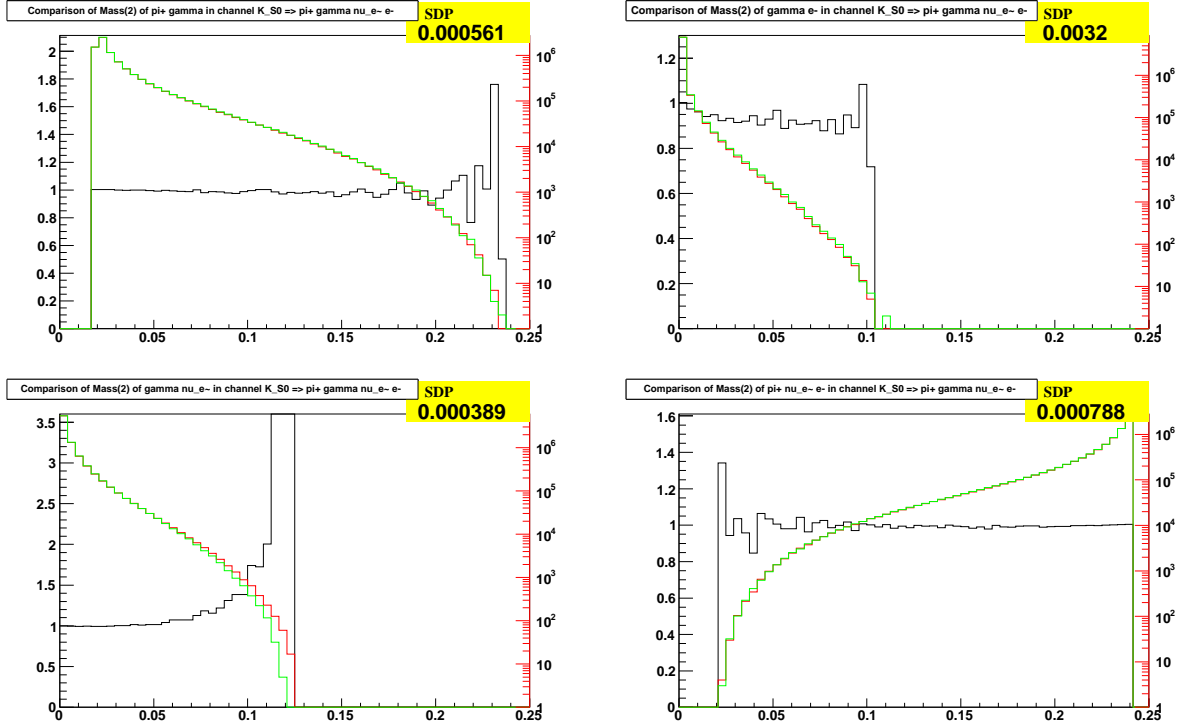


Figure 6: Distributions of scalar Lorentz invariants, in  $\text{GeV}^2$  units, constructed from the decay products in  $K^0 \rightarrow \pi^+ e^- \nu_e$  channel. Invariants most sensitive to photon energy are plotted. Single kinematical branch is used, thus the phase space is exact. The red (darker grey) line is standard PHOTOS, the green is with exact Matrix Element, both correspond to the right logarithmic scale. The black line is ratio of red to green, and correspond to the left linear scale. The fraction of accepted bremsstrahlung events is  $8.6398 \pm 0.0029 \%$  in standard PHOTOS run and  $8.6958 \pm 0.0029 \%$  for the case where the matrix element is used.

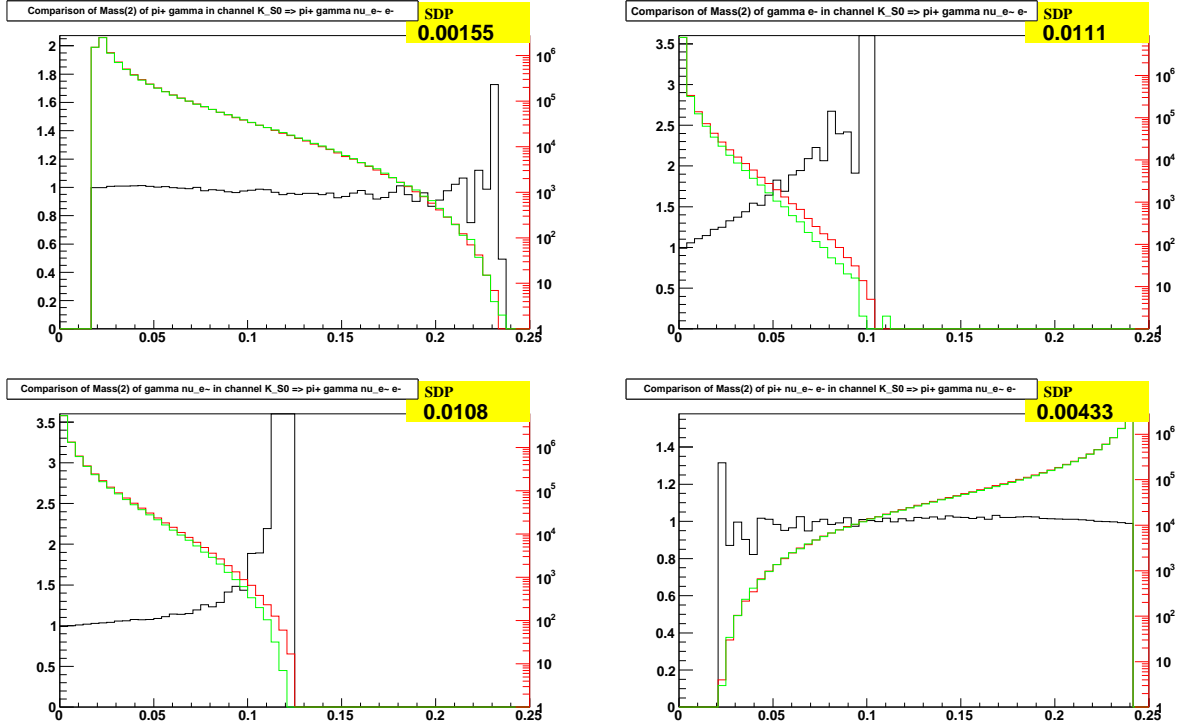


Figure 7: Distributions of scalar Lorentz invariants, in  $\text{GeV}^2$  units, constructed from the decay products in  $K^0 \rightarrow \pi^+ e^- \nu_e$  channel. Invariants most sensitive to photon energy are plotted. Single kinematical branch is used, thus the phase space is exact. The red (darker grey) line is standard PHOTOS, the green is with exact Matrix Element, both correspond to the right logarithmic scale. The black line is ratio of red to green, and correspond to the left linear scale. The fraction of accepted bremsstrahlung events is  $8.6398 \pm 0.0029 \%$  in standard PHOTOS run and  $8.5235 \pm 0.0029 \%$  for the case when matrix element from Ref. [17] is used.



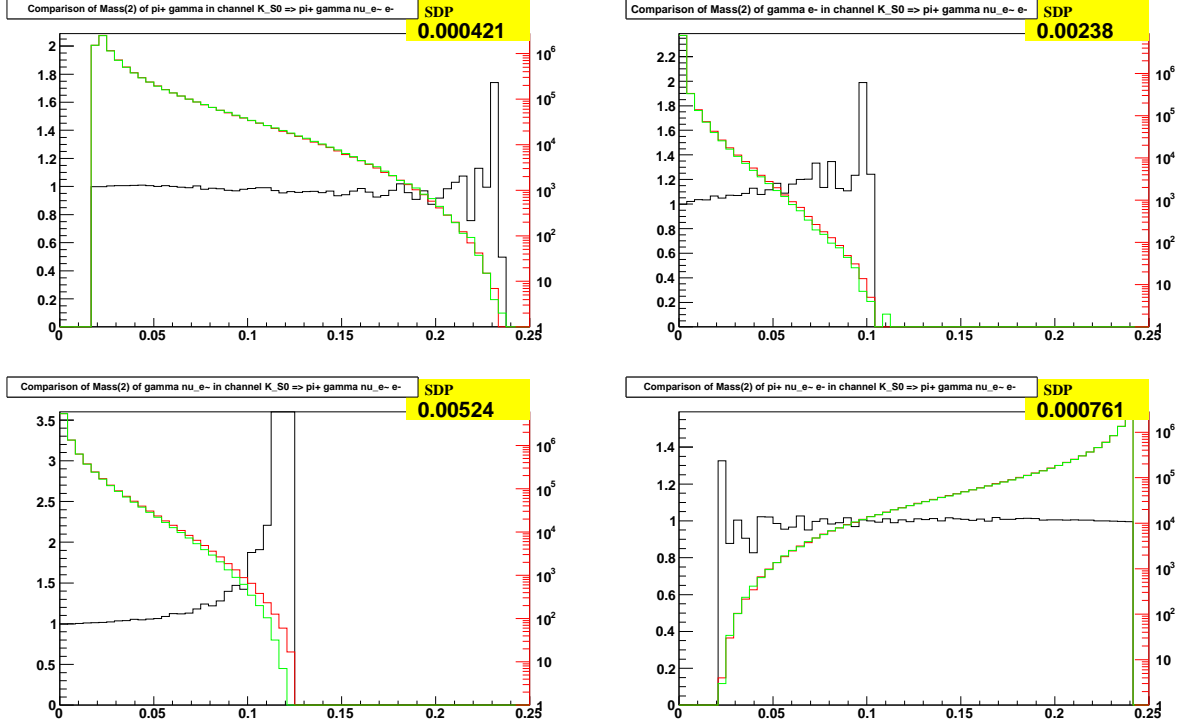


Figure 8: Distributions of scalar Lorentz invariants, in  $\text{GeV}^2$  units, constructed from the decay products in  $K^0 \rightarrow \pi^+ e^- \nu_e$  channel. Invariants most sensitive to photon energy are plotted. Single kinematical branch is used, thus the phase space is exact. The red (darker grey) line is standard PHOTOS, the green is with exact Matrix Element, both correspond to the right logarithmic scale. The black line is ratio of red to green, and correspond to the left linear scale. The fraction of accepted bremsstrahlung events is  $8.6398 \pm 0.0029 \%$  in standard PHOTOS run and  $8.5928 \pm 0.0029 \%$  for the case when matrix element of Ref. [17] with improvement of formula (22) is used.

## 6 Summary

In this study we have adopted the matrix element of [17] and of scalar QED for the emission kernel of PHOTOS Monte Carlo [7, 8, 10]. We have investigated decays of Kaons into  $\pi$  and lepton neutrino pair. After modification for these channels, PHOTOS features exact matrix element (three options) and exact phase space. We have evaluated the numerical size of the terms missing in publicly available version of PHOTOS. The difference is of the order of 0.2 %, thus rather small, except for the distribution of lepton photon pair invariant mass spectrum, where the difference is sizable at the high end of the spectrum in case of  $K^0$  decay. We have investigated the main source of the differences between matrix element of scalar QED and of [17] as well. We have found that the dominant source of the differences originate from phase space regions where the photon direction is close to that of  $\pi^\pm$ . After adjustment of the terms, formally representing corrections due to leading logarithms of  $\pi^\pm$  mass, the difference got reduced by a factor of 2 to 4, depending on the distribution. These obviously non-leading effects may be nonetheless of interest, if the calculations would be applied to decays of  $B$  mesons.

On the technical side, we have also checked the algorithm. We have compared the case when the pre-sampler is active for possible collinear singularity along lepton only (for which the phase space is exact and phase-space Jacobians are explicit), and the case when both pre-samples for singularities along lepton and charged  $\pi$  directions are active. Such studies for more than 2 body decays were not documented until now. We found the differences to be below 0.05 %. Our paper is supplemented with a larger set of figures, which are available from the web-page [23].

We conclude that for PHOTOS version 2.15 or higher, and for  $K_{l3}$  decays, the precision level with respect to matrix elements based simulation is 0.2% or better. This conclusion extends naturally to the case of multiple photon emission. We found the factorization properties of matrix element, which are necessary for that purpose. On the other hand, our error estimation is not complete. It does not include discussion of uncertainty in the matrix elements due to assumptions of the models used for their calculation. Also, non leading effects of virtual corrections, which are expected to contribute at 0.2 % level, are not discussed. They depend on the details of hadronic interactions and can not be tackled in discussion of bremsstrahlung only.

### Acknowledgements

We would like to thank Tomasz Przedzinski for the help in obtaining the numerical results presented in in this paper.

## References

- [1] M. Antonelli, V. Cirigliano, G. Isidori, F. Mescia, M. Moulson, *et al.*, *Eur.Phys.J.* **C69** (2010) 399–424, 1005.2323.
- [2] S. Actis *et al.*, *Eur. Phys. J.* **C66** (2010) 585–686, 0912.0749.

- [3] D. R. Yennie, S. Frautschi, and H. Suura, *Ann. Phys. (NY)* **13** (1961) 379.
- [4] S. Jadach and B. F. L. Ward, *Phys. Rev.* **D38** (1988) 2897.
- [5] S. Jadach, Z. Wąs, and B. F. L. Ward, *Comput. Phys. Commun.* **130** (2000) 260, Up to date source available from <http://home.cern.ch/jadach/>.
- [6] E. Barberio, B. van Eijk, and Z. Wąs, *Comput. Phys. Commun.* **66** (1991) 115.
- [7] E. Barberio and Z. Wąs, *Comput. Phys. Commun.* **79** (1994) 291–308.
- [8] P. Golonka and Z. Was, *Eur. Phys. J.* **C45** (2006) 97–107, [hep-ph/0506026](#).
- [9] P. Golonka and Z. Was, *Eur. Phys. J.* **C50** (2007) 53–62, [hep-ph/0604232](#).
- [10] G. Nanava and Z. Was, *Eur. Phys. J.* **C51** (2007) 569–583, [hep-ph/0607019](#).
- [11] G. Nanava, Q. Xu, and Z. Was, *Eur.Phys.J.* **C70** (2010) 673–688, [0906.4052](#).
- [12] N. Davidson, G. Nanava, T. Przedzinski, E. Richter-Was, and Z. Was, [1002.0543](#).
- [13] M. E. Peskin and D. V. Schroeder, *An Introduction to Quantum Field Theory*, Westview Press, 1995.
- [14] S. Weinberg, *Physica* **A96** (1979) 327, Festschrift honoring Julian Schwinger on his 60th birthday.
- [15] J. Gasser and H. Leutwyler, *Annals Phys.* **158** (1984) 142.
- [16] H. Leutwyler, *Annals Phys.* **235** (1994) 165–203, [hep-ph/9311274](#).
- [17] V. Cirigliano, M. Giannotti, and H. Neufeld, *JHEP* **0811** (2008) 006, [0807.4507](#).
- [18] V. Cirigliano, *PoS KAON* (2008) 007.
- [19] Y. Bystritskiy, S. Gevorkyan, and E. Kuraev, *Eur.Phys.J.* **C64** (2009) 47–54, [0906.0516](#).
- [20] M. Jezabek, Z. Wąs, S. Jadach, and J. H. Kühn, *Comput. Phys. Commun.* **70** (1992) 69.
- [21] P. Golonka, T. Pierzchala, and Z. Was, *Comput. Phys. Commun.* **157** (2004) 39–62, [hep-ph/0210252](#).
- [22] N. Davidson, P. Golonka, T. Przedzinski, and Z. Was, *Comput. Phys. Commun.* **182** (2011) 779–789, [0812.3215](#).
- [23] <http://wasm.web.cern.ch/wasm/newprojects.html>  
<http://hibiscus.if.uj.edu.pl/~przedzinski/Kl3/>.

- [24] Particle Data Group Collaboration, K. Nakamura *et al.*, *J. Phys.* **G37** (2010) 075021.
- [25] NA48/2 Collaboration, J. R. Batley *et al.*, *Eur. Phys. J.* **C50** (2007) 329–340, [hep-ex/0702015](#).
- [26] N. Davidson, T. Przedzinski, and Z. Was, [1011.0937](#).